Appl. Phys. B (2013) 111:559–565
DOI 10.1007/s00340-013-5373-x

Applied Physics B
Lasers and Optics

Generation of high-energy broadband femtosecond deep-ultraviolet pulses by highly nondegenerate noncollinear four-wave mixing in a thin transparent solid

Rosa Weigand · Helder M. Crespo

Received: 22 August 2012 / Accepted: 8 February 2013 / Published online: 21 March 2013

Abstract We present a simple and efficient technique for the generation of ultrashort deep-ultraviolet pulses based on four-wave mixing of noncollinear laser pulses in a thin solid. Sub-30-fs pulses (Fourier-limit of 13 fs) centered at 270 nm, with energies up to 6 μJ, were obtained by mixing the fundamental and the second harmonic of a Ti:sapphire amplifier in fused silica. Temporal characterization was performed with a dispersionless self-diffraction FROG setup. Spectra as broad as 20 nm were also obtained that can in principle support sub-4-fs deep-ultraviolet pulses.The results are well described by two-dimensional numerical simulations.

1 Introduction

The availability of sub-300-nm deep ultraviolet (DUV) ultrashort pulses with microjoule energies enables many experimental studies of ultrafast processes in photophysics, photochemistry and photobiology [1], and is relevant for precision laser processing of materials [2].

The efficient generation of intense sub-30-fs DUV radiation is a challenging task and a topic of intense research. Several techniques based on four-wave mixing (FWM) in gaseous media have been employed, from third-order difference-frequency generation (DFG) of Ti:-Sapphire laser pulses and their second harmonic (SH) in hollow waveguides [3, 4] and in filaments [5, 6], to DFG of pre-chirped pulses in complex dual hollow-fiber systems [7]. Other techniques include compression after spectral broadening in a gas-filled hollow fiber of the third harmonic (TH) of a Ti:sapphire amplifier that has been further amplified by an excimer system [8], spectral broadening during filamentation in gas of TH pulses from a high-energy dual-stage amplifier [9], and direct harmonic upconversion of few-cycle femtosecond pulses in gases [10, 11]. This last method has enabled the generation of the shortest (sub-3-fs) DUV pulses to date [12]. These techniques typically result in DUV pulses with energies ranging from several hundred nanojoule up to a few microjoule [3, 4, 5, 6, 7, 10, 11, 12], and even a few hundred microjoule [8, 9], but in general require complicated and/or large setups and involve the use and handling of gases. Ultrashort DUV pulses can also be generated in condensed matter by nonlinear wave mixing in $\chi^{(2)}$ crystals, but reaching sub-30-fs pulses requires relatively complex techniques, such as frequency doubling of a noncollinear optical parametric amplifier (NOPA) in thin BBO crystals [13] or using a broadband achromatic setup [14].

In previous work, we reported on the generation of multiple upconverted pulses with wavelengths down to 209 nm in fused silica by noncollinear cascaded four-wave mixing (CFWM) [15] of the 615- and 569-nm beams from a dye laser-amplifier [16], although wavelengths below 300 nm were limited to sub-microjoule energies. Other authors also used noncollinear FWM of cylindrically focused beams in fused silica to obtain 10 μJ, 33 fs near-DUV pulses at 310 nm with 2 % pump to DUV efficiency from a 400-nm pump pulse and a chirped 560 nm idler

R. Weigand (✉)
Departamento de Óptica, Facultad de Ciencias Físicas,
Universidad Complutense de Madrid,
Avda. Complutense s/n, 28040 Madrid, Spain
e-mail: weigand@fis.ucm.es

H. M. Crespo
IFIMUP/IN and Departamento de Física e Astronomia,
Faculdade de Ciências, Universidade do Porto,
Rua do Campo Alegre 687, 4169-007 Porto, Portugal
e-mail: hcrespo@fc.up.pt

pulse generated in a NOPA [17]. Although these techniques are based on solid-state nonlinear media, they still require complex and relatively large setups or involve a less common laser source. Therefore, a compact, low-cost system for generating microjoule level sub-30-fs DUV pulses would be an interesting alternative in many laboratories already equipped with more common laser amplifiers.

In this paper, we present a practical, simple and efficient source of intense broadband DUV femtosecond pulses based on highly nondegenerate noncollinear FWM, in a thin solid, of the fundamental and SH pulses from a Ti:sapphire laser amplifier.

2 Experimental setup and results

The experimental setup is shown in Fig. 1. A multipass amplifier (Femtopower Compact Pro CEP, Femtolasers GmbH) provides <1 mJ, ~27 fs, horizontally polarized pulses with a central wavelength of 800 nm (the fundamental frequency ω) at a repetition rate of 1 kHz. The beam is reduced with a refractive telescope down to a 5-mm spot and a type-I 200-μm thick BBO crystal generates the SH at 400 nm (2ω). The chirp of the fundamental beam was adjusted to optimize the conversion efficiency, which reached ~40 % with a bandwidth capable of supporting ~30 fs pulses. A dichroic mirror (DM) separates the residual fundamental beam from the SH beam and a half-wave plate rotates the polarization plane of the fundamental beam by 90°. The resulting s-polarized fundamental and SH beams are then sent with aluminum mirrors (M1-M3) and 45° ultrafast dielectric mirrors (M4–M8) towards focusing lenses L1 (fused silica, f = 300 mm at 400 nm) and L2 (BK7, f = 265 mm at 800 nm), respectively (see Fig. 1). These lenses focus the beams in a thin slide of fused silica (150 or 500 μm thick) with an external interaction angle $\theta = 23.2°$ (corresponding to an internal angle of 15.75°) which provides geometrical phase-matching for the four-wave difference-frequency mixing process $3\omega = 2 \times (2\omega) - \omega$ that generates radiation around 266 nm [15, 19]. Lenses were used instead of reflecting optics because they provide much more flexibility in terms of adjusting the beam fluence in the nonlinear medium independently of other relevant beam parameters, namely interaction angle, although at the cost of some additional dispersion. Note that if mirrors were used instead of lenses this by itself would not suffice to achieve transform-limited pulses at the plane of the sample. In fact, since it is important to have minimum pulse duration at the plane of the SHG crystal (for maximum conversion efficiency), we optimized the amplifier compressor using this criterion. This however meant that, to have transform-limited pulses at the plane of the fused silica slide, we would have to additionally and independently compensate for the dispersion experienced by both the fundamental and the SHG beams in the beamsplitter substrate and coatings, as well as in the air paths. The use of mirrors as focusing elements would not prevent this, even though overall dispersion would be less than compared to lenses. Such a setup could give the impression that to generate broadband pulses, the fundamental and SHG pulses would have to be compressed first, at the expense of a significant increase in experimental complexity, which is not the case. So the use of lenses is the simplest and more

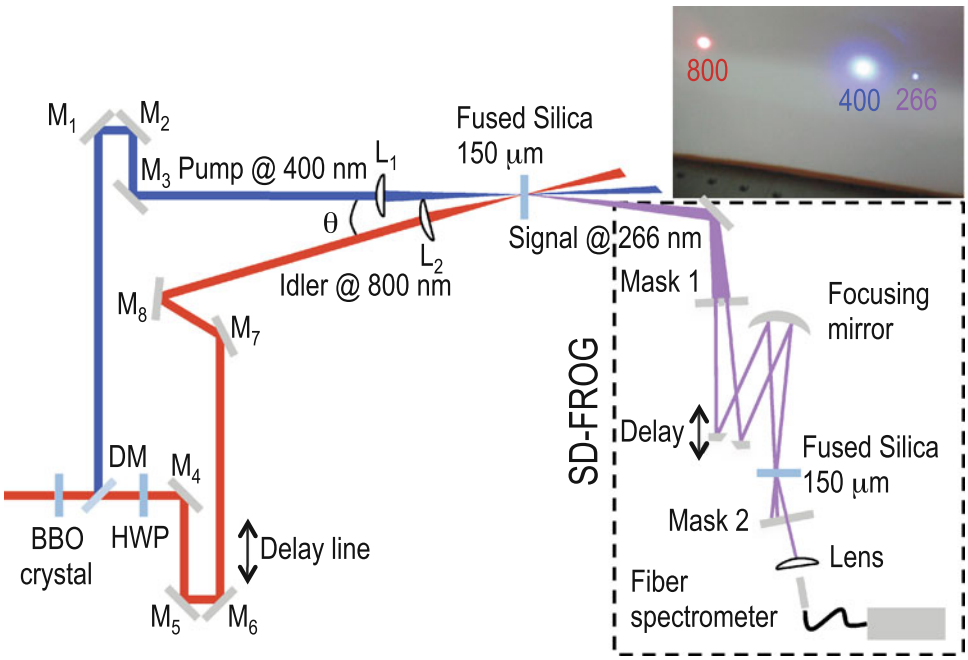

Fig. 1 Experimental setup for ultrashort DUV pulse generation and temporal characterization. DM dichroic mirror, HWP half-wave plate, M1–M3 aluminum mirrors, M4–M8 45° dielectric mirrors. *Inset* idler, pump and generated DUV beam, directly projected onto a white card

practical and flexible option. The measured energies at the plane of the slide were 314 μJ for the ω pulse and 171 μJ for the 2ω pulse. Assuming the fundamental beam is compressed at the BBO crystal (since the conversion efficiency was optimized), the pulse is temporally stretched by the DM substrate and the 5-mm glass thickness of the focusing lens to ~50 fs. The FWHM duration of the 2ω pulse was measured with the self-diffraction FROG setup described below and amounted to 48.6 fs (FROG error of 0.0029 for a 256 × 256 grid; time-bandwidth product of 0.52). We see that both the fundamental and SH pulses have some positive chirp, as expected, which was not compensated for. In order to avoid optical damage to the sample and to maintain good beam quality, the slide was placed approximately 2 cm before the focus of the lenses. Assuming the incident beams are at a waist in the plane of the lenses, the estimated intensities of the fundamental and second harmonic pulses at the plane of the sample were 2.6×10^{12} and 1.2×10^{12} W/cm^2, respectively. Synchronization was achieved with a delay line in the fundamental beam.

For the 150-μm slide, we obtained intense DUV pulses emitted at an angle of ~7° with respect to the 400-nm beam (see inset of Fig. 1) with energies of 5–6 μJ, as measured with a calibrated broadband power meter (pump-to-signal conversion efficiency of ~3 %). The resulting efficiency is comparable to that of techniques based on FWM in gases [3, 4, 5, 6]. The calculated group velocity mismatch length for the noncollinear pump and idler pulses in fused silica is approximately 1 mm, so one could expect the DUV generation to be more efficient for a thicker medium. However, the energies obtained for the 500-μm slide were only slightly higher (6–7 μJ) than for the 150-μm slide and the beam quality was worse due to a correspondingly higher transverse phase modulation. The observed limitation in efficiency could be due to an intensity-induced time-dependent phase mismatch in the FWM process, as described in detail in [20] and suggested in [17]. Therefore, all following measurements concern the 150-μm slide alone.

The generated DUV spectra were measured with a fiber coupled spectrometer equipped with a 400-μm core fiber. Figure 2 shows the typical spectra obtained for different delays (separated by ~33 fs) between idler and pump pulses. As mentioned above, the energy obtained for the more intense pulses (0 fs delay) was 5–6 μJ. Weaker pulses are more difficult to measure directly, so we opted to perform an integration of the measured spectra (in frequency). Taking the stronger spectrum as reference with 6 μJ we obtained 1.5, 2.4, 3.85, 6, 4.75, 4.9 and 1.4 μJ for the delays ranging from −99 to 99 fs, respectively. The observed dependence of the spectral shape and central wavelength of the generated DUV pulses on the delay is due to cross-phase modulation between the pump and idler pulses (blue-shift when the blue pump arrives after the more intense red idler and experiences the latter's trailing edge). Figure 3 shows the widest spectrum obtained with our setup for slightly higher intensities than those used in Fig. 2. It has a bandwidth of ~20 nm and in principle could support sub-4-fs (sech^2) pulses, provided that its phase can be properly compensated for. The beam quality of the DUV pulse was good enough to induce significant spectral broadening by self-phase modulation in a second fused silica slide. Broader bandwidth DUV pulses also tend to have more complex spatial profiles, so we chose to achieve a compromise between beam profile and spectral width by adjusting the pump and idler intensities and the delay.

The resulting DUV pulses were temporally characterized with a self-diffraction FROG (SD-FROG) setup similar to those described in [3, 11] (see Fig. 1). The DUV beam was sent through a first mask consisting of two orifices with 1.6 mm diameter separated by 3.5 mm, placed so that the portions of the beam transmitted through each hole had similar intensities. The delay between the two transmitted pulses was controlled with a pair of d-shaped

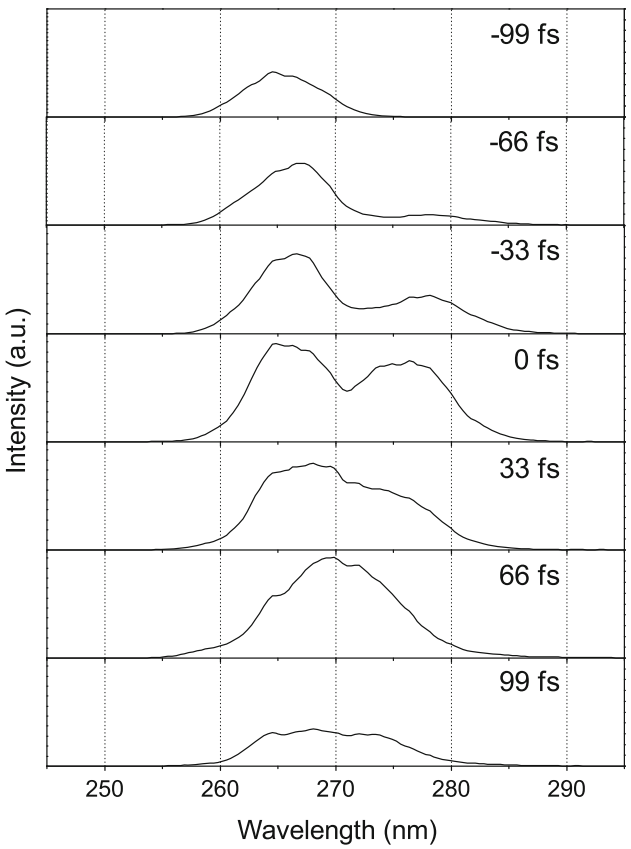

Fig. 2 Experimental spectra of the generated DUV signal for different delays (separated by ~33 fs) between idler and pump pulses. Negative delay: pump arrives after idler, positive delay: pump arrives before idler

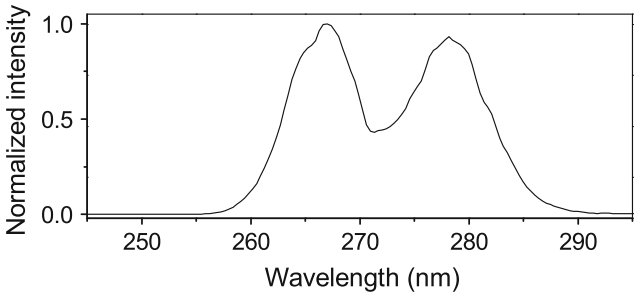

Fig. 3 Broadest experimental spectrum obtained in our setup

mirrors and a stepper motor stage (3.33 fs step size). The pulses were focused by a spherical aluminum mirror (f = 200 mm) in a second 150 μm fused silica slide, where the image of the orifices was formed, and the generated self-diffraction signal was isolated with a second mask prior to coupling to the spectrometer.

The measured and retrieved SD-FROG traces are given in Fig. 4a, b, and the temporal profile and spectrum of the pulses (retrieved with Femtosoft FROG software) are shown in Fig. 4c, d; the FROG error was 0.005 for a 256 × 256 grid. We obtained good quality 27.3 fs DUV pulses with a spectral width of 5.7 nm and a time-bandwidth product of 0.67. This duration is roughly a factor of 2 larger than what could in principle be achieved. Still, the pulses show mostly linear chirp, which is due to the uncompensated chirp in the pump pulse, the dispersion of air in the setup, and the self-phase and cross-phase modulation process (as will be shown numerically below), which means that they could be further compressed. The transform-limited duration for the 5.7-nm wide spectrum assuming a sech^2 shape is 12.8 fs.

3 Simulation

To further validate and understand the experimental results, a 2D model developed within our group was used to calculate

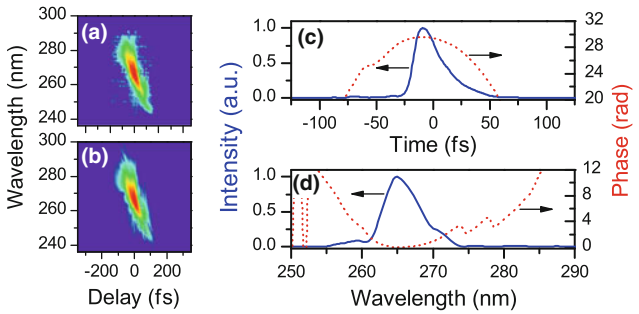

Fig. 4 **a** Experimental and **b** retrieved SD-FROG traces of the DUV pulses (in *log scale*); **c** retrieved pulse in the time and **d** frequency domains

the main characteristics and behavior of the measured DUV pulses. This model has been described elsewhere [18, 19] and considers nonlinear pulse propagation, within the slowly varying envelope approximation, of the noncollinearly interacting gaussian-shaped (in space and time) pump and idler beams, in the 2D plane defined by their wavevectors $\mathbf{k}_{2\omega}$ and $\mathbf{k}_{\omega}$, respectively. The model includes terms for phase modulation, diffraction, dispersion and self-steepening which proved to be sufficient to successfully reproduce the main characteristics of the beams generated by cascaded four-wave mixing in bulk solids characterized by a purely real, nonresonant $\chi^{(3)}$ nonlinearity [18, 19].

As input parameters the model needs the central wavelength, temporal shape and duration of the pump (2ω) and idler (ω) beams, their intensities at the plane of the medium, their interaction angle θ inside the medium, their relative delay and relative transverse position at the entrance of the medium. The medium is described by its thickness and its linear and nonlinear refractive indices in the desired spectral range. This model has permitted us to calculate the spectra, temporal duration and emission angle of the cascaded four-wave mixing generated beams, as well as the energy efficiency of the up- and down-converted pulses, in very good agreement with the experimental results [18]. Here we have applied it to calculate the spectrum, spectral phase, energy efficiency, duration and emission angle of the generated DUV pulses.

In the simulations, we assumed transform-limited input pulses with durations $t_{2\omega} = 50$ fs and $t_{\omega} = 50$ fs and central wavelengths $\lambda_{2\omega} = 400$ nm and $\lambda_{\omega} = 800$ nm for the pump and idler pulses, respectively. The intensities were $I_{\omega} = 2.6 \times 10^{12}$ W/cm^2 and $I_{2\omega} = 1.2 \times 10^{12}$ W/cm^2. The interaction angle between the pulses was set at $\theta = 15.0°$, 15.7°(perfect phase-matching) and 16.4°. The relative transverse spatial offset of the beams at the entrance of the medium was 10 μm to maximize their spatial overlap inside the medium.

Figure 5 shows the simulated DUV spectra as a function of the relative delay between pump (ω) and idler (2ω) pulses for $\theta = 15.0°$ (slightly smaller than the perfect phase-matching angle). We see that the general features and overall behavior of the simulated spectra are in good agreement with the experimental observations. In particular, the spectra show a double-band structure in which its bluer portion is enhanced for negative delays (more intense idler arrives before weaker pump) while its redder portion becomes more intense for positive delays (idler arrives after pump). The two situations are of course not symmetrical because of the different group velocities of the pulses, where the idler can catch up with the pump in situations of positive delay but will always come before the pump for negative delays. Regarding the spectral phases we see that, even though the input pulses are transform-

limited, the generated DUV pulses have chirp. Moreover, the broadest generated DUV pulses (delays of −20, 0 and 20 fs in Fig. 5) have a clear positive chirp, due the self- and cross-phase modulation-induced spectral broadening that occur simultaneously with the nondegenerate FWM process. This result is consistent with the observed chirp in the measured pulses (see Fig. 4). For 0 fs delay between pump and idler pulses, we calculate an emission angle of 7.3°, an output energy efficiency of 3.6 % with respect to the pump pulse, and a pulse width of 19.7 fs (9 fs TL duration), in very reasonable agreement with the measurements.

Figures 6 and 7 show the numerical results obtained for interaction angles $\theta = 15.7°$ (perfect phase-matching) and $\theta = 16.4°$, respectively, using the same intensities as in Fig. 5. Although higher energy efficiencies are obtained at 0 fs delay for both interaction angles than in the case of $\theta = 15.0°$ (12.5 and 6.9 % with respect to the pump pulse for $\theta = 15.7°$ and $\theta = 16.4°$, respectively), the corresponding spectral widths are narrower. The configuration of perfect phase-matching angle produces single-peaked bands narrower than those obtained in the experiment and in Fig. 5. The case of slightly larger angle $\theta = 16.4°$ can produce spectra even more shifted to the blue, but again the spectral bandwidths are narrower than in the case of Fig. 5, which seems to better represent the actual experimental configuration (experimentally, the interaction angle was optimized to maximize the spectral width of the generated DUV pulses). For both cases, the behavior of the spectral phases is similar to the one obtained in Fig. 5.

Since we are using a non-collinear interaction geometry, with rather large angles between the interacting beams, the generated pulse has angular chirp, since the different frequencies will be generated at different angles, due to the phase matching condition. To estimate the typical amount of angular chirp in the generated DUV beam, we have calculated the angle at which each frequency is generated

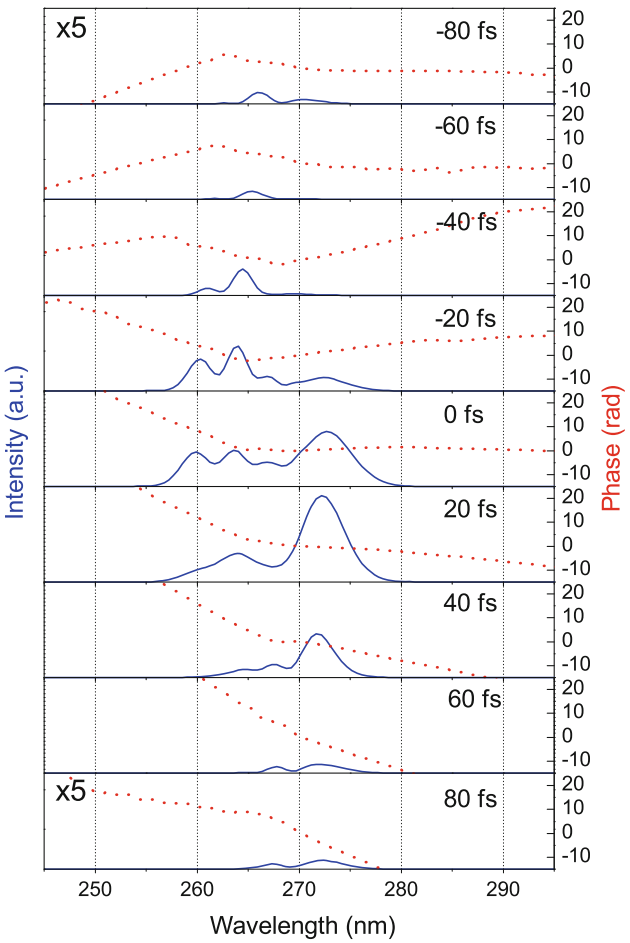

Fig. 5 Simulated spectral intensity and phase of the generated DUV signal for $\theta = 15.0°$ and different delays between idler and pump pulses (the intensities in the first and the last plots have been multiplied by a factor of 5). Negative delay: idler arrives before pump, positive delay: idler arrives after pump

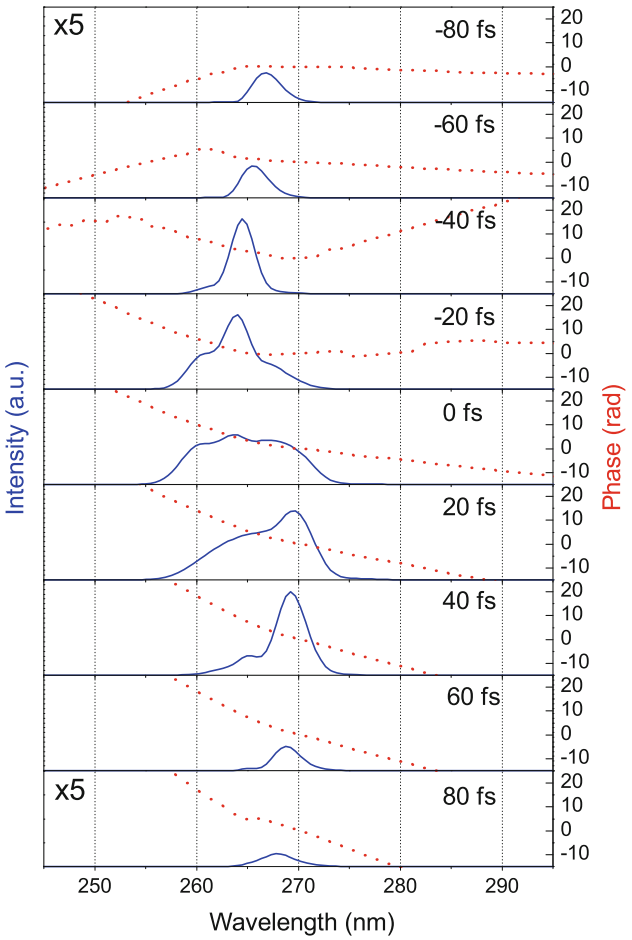

Fig. 6 Simulated spectral intensity and phase of the generated DUV signal for $\theta = 15.7°$ and different delays between idler and pump pulses (negative and positive delays as in Fig. 5, note the scale factors for the first and last intensity plots)

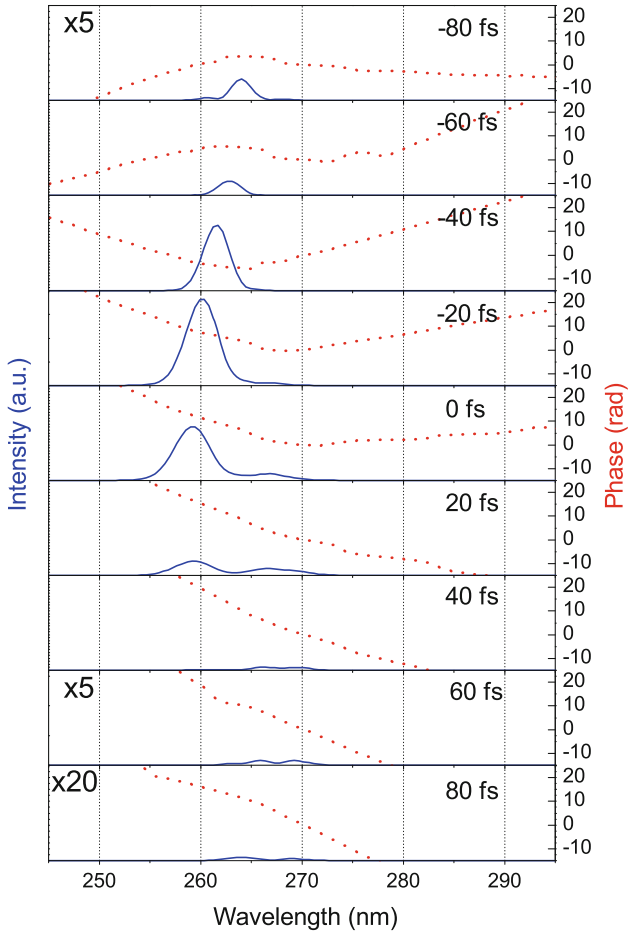

Fig. 7 Simulated spectral intensity and phase of the generated DUV signal for $\theta = 16.4°$ and different delays between idler and pump pulses (negative and positive delays as in Fig. 5, note the scale factors for the first and last two intensity plots)

for the case of 0 fs delay of Fig. 5 and the results are shown in Fig. 8. From the figure, we see that the spectrum (spanning from 255 to 280 nm) is spread across a small angle of approximately 0.5°, or less than 9 mrad. This is sufficiently small for many practical applications. Also, since the different frequencies originate from a relatively small region in the thin medium, it should be possible to spatially recombine the spectrum using focusing optics, as we have done in our XFROG setup, which has enabled us to properly gate the full spectrum of the pulses.

It would also be very interesting if very short DUV pulses could be generated starting from transform-limited fundamental and second-harmonic pulses with durations around 100 fs, which are available in many laboratories. We studied this possibility numerically, first using a pair of Gaussian transform-limited 100 fs pulses with an interaction angle of 15.0°, zero relative delay and intensities equal to those previously used in the experiments and simulations ($I_\omega = 2.6 \times 10^{12}$ W/cm^2 and $I_{2\omega} = 1.2 \times 10^{12}$ W/cm^2). In this case, we obtained transform-limited DUV pulses

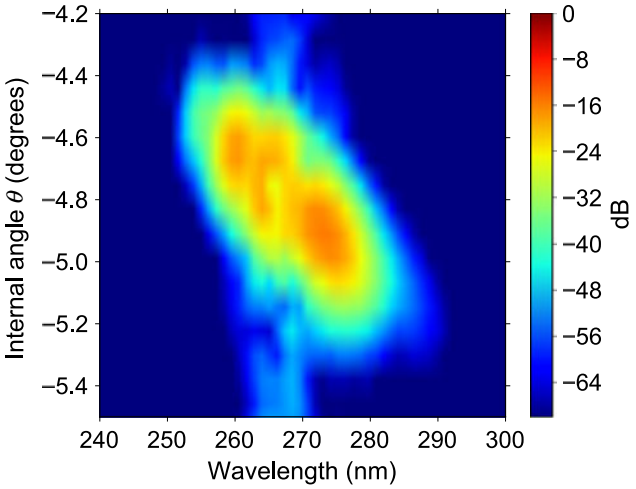

Fig. 8 Angular chirp of the generated beam for the case of 0 fs delay in Fig. 5. The intensity is given in dB with respect to the maximum intensity of the pump pulses

with a duration of 42 fs. We found that further optimization of the pump intensities to $I_\omega = 2.0 \times 10^{12}$ W/cm^2 and $I_{2\omega} = 2.0 \times 10^{12}$ W/cm^2 resulted in the generation of 29.5 fs DUV pulses. Therefore, it seems possible (at least numerically) to obtain sub-30-fs pulses starting from 100 fs pump pulses using this technique. Further work in this context will be done in the future.

4 Conclusion

In conclusion, we have experimentally demonstrated the efficient generation of broadband DUV pulses with 27.6 fs (compressible to ~13 fs) and energies up to 6 μJ using a simple scheme of highly nondegenerate four-wave mixing in a thin transparent solid of the fundamental and SH pulses from a Ti:sapphire laser amplifier; the generated pulses were characterized with a dispersionless SD-FROG setup. The results are well described by two-dimensional numerical simulations using transform-limited pump and idler pulses. The broadest experimentally generated spectra, up to 20 nm wide (FWHM), show promise for the generation of sub-4-fs DUV pulses. Due to its simplicity, this technique should be useful in many fields and laboratories interested in implementing an efficient source of ultrashort high-energy DUV pulses.

Acknowledgments This work was supported in part by Acción Integrada HP2008-0064 from MICINN in Spain, Fundação das Universidades Portuguesas in Portugal, and Fundos FEDER, through Programa Operacional Factores de Competitividade - COMPETE and Fundação para a Ciência e Tecnologia (FCT) under grants PTDC/FIS/115102/2009 and PTDC/FIS/122511/2010. R. Weigand acknowledges permission for a sabbatical leave from Universidad Complutense de Madrid. We also thank João L. Silva for his help with the simulation code.

References

1. I. Hertel, W. Radloff, Rep. Progr. Phys. **69**, 1897 (2006)
2. H.J. Klein-Wiele, J. Bekesi, P. Simon, Appl. Phys. A **79**, 775 (2004)
3. G.C. Durfee, S. Backus, H.C. Kapteyn, M.M. Murnane, Opt. Lett. **24**, 697 (1999)
4. E.A. Jailaubekov, E.S. Bradforth, Appl. Phys. Lett. **87**, 021107 (2005)
5. T. Fuji, T. Horio, T. Suzuki, Opt. Lett. **32**, 2481 (2007)
6. T. Fuji, T. Suzuki, E.E. Serebryannikov, A. Zheltikov, Phys. Rev. A **80**, 063822 (2009)
7. Y. Kida, J. Liu, T. Teramoto, T. Kobayashi, Opt. Lett. **35**, 1807 (2010)
8. T. Nagy, P. Simon, Opt. Lett. **34**, 2300 (2009)
9. M. Ghotbi, P. Trabs, M. Beutler, Opt. Lett. **36**, 463 (2011)
10. S. Backus, J. Peatross, Z. Zeek, A. Rundquist, G.Taft, M.M. Murnane, H.C. Kapteyn, Opt. Lett. **21**, 665 (1996)
11. U. Graf, M. Fiess, M. Schultze, R. Kienberger, F. Krausz, E. Goulielmakis, Opt. Express **16**, 18956 (2008)
12. F. Reiter, U. Graf, M. Schultze, W. Schweinberger, H. Schröder, N. Karpowicz, A. Azzeer, R. Kienberger, F. Krausz, E. Goulielmakis, Opt. Lett. **35**, 2248 (2010)
13. M. Beutler, M. Ghotbi, F. Noack, D. Brida, C. Manzoni, G. Cerullo, Opt. Lett. **34**, 710 (2009)
14. P. Baum, S. Lochbrunner, E. Riedle, Opt. Lett. **29**, 1686 (2004)
15. H. Crespo, J. Mendonça, A. Dos Santos, Opt. Lett. **25**, 829 (2000)
16. R. Weigand, T.J. Mendonça, H.M. Crespo, Phys. Rev. A **79**, 063838 (2009)
17. J. Darginavičius, G. Tamošauskas, A. Piskarkas, A. Dubietis, Opt. Express **18**, 16096 (2010)
18. J. Silva, R. Weigand, H. Crespo, Opt. Lett. **34**, 2489 (2009)
19. J. Silva, H. Crespo, R. Weigand, Appl. Opt. **50**, 1968 (2011)
20. A. Penzkofer, H.J. Lehmeier, Opt. Quantum Electron. **25**, 815 (1993)